New Analytical Potential Energy Surface for the $F(^2P) + CH_4$ Hydrogen Abstraction Reaction: Kinetics and Dynamics

J. Espinosa-García,* J. L. Bravo, and C. Rangel

Departamento de Química Física, Universidad de Extremadura, 06071 Badajoz, Spain

Received: December 22, 2006; In Final Form: February 8, 2007

A new potential energy surface for the gas-phase $F(^2P) + CH_4$ reaction and its deuterated analogues is reported, and its kinetics and dynamics are studied exhaustively. This semiempirical surface is completely symmetric with respect to the permutation of the four methane hydrogen atoms, and it is calibrated to reproduce the topology of the reaction and the experimental thermal rate constants. For the kinetics, the thermal rate constants were calculated using variational transition-state theory with semiclassical transmission coefficients over a wide temperature range, 180−500 K. The theoretical results reproduce the experimental variation with temperature. The influence of the tunneling factor is negligible, due to the flattening of the surface in the entrance valley, and we found a direct dependence on temperature, and therefore positive and small activation energies, in agreement with experiment. Two sets of kinetic isotope effects were calculated, and they show good agreement with the sparse experimental data. The coupling between the reaction coordinate and the vibrational modes shows qualitatively that the FH stretching and the CH_3 umbrella bending modes in the products appear vibrationally excited. The dynamics study was performed using quasi-classical trajectory calculations, including corrections to avoid zero-point energy leakage along the trajectories. First, we found that the FH(v',j') rovibrational distributions agree with experiment. Second, the excitation function presents an oscillatory pattern, reminiscent of a reactive resonance. Third, the state specific scattering distributions present reasonable agreement with experiment, and as the FH(v') vibrational state increases the scattering angle becomes more forward. These kinetics and dynamics results seem to indicate that a single, adiabatic potential energy surface is adequate to describe this reaction, and the reasonable agreement with experiment (always qualitative and sometimes quantitative) lends confidence to the new surface.

I. Introduction

The polyatomic $F(^2P) + CH_4 \rightarrow FH(v') + CH_3$ reaction has special theoretical and experimental interest because of the FH(v') vibrational population inversion produced in this reaction, which constitutes a chemical laser system.

Our group has given much attention to this reaction in recent years. In 1996, we reported[1] for the first time an analytical potential energy surface (PES) for the title reaction (PES-1996), which was modified and updated in 2005[2] to correct its deficiencies. This last surface was symmetric with respect to any permutation of the four methane hydrogen atoms, and was calibrated to reproduce the experimental rate constants. To analyze the effect of the spin−orbit electronic states of the fluorine atom, $^2P_{3/2}$ and $^2P_{1/2}$, two versions were constructed, called PES-SO and PES-NOSO; it was found that the latter reproduces better the experimental kinetics measurement. This PES-NOSO surface is called PES-2005 in the present paper. In both surfaces, PES-1996 and PES-2005, the studies focused on kinetics aspects, such as forward rate constants and kinetic isotope effects (KIEs). Shortly after we had constructed the PES-2005 surface, two dynamics studies using quasi-classical trajectory (QCT) calculations[3,4] questioned the suitability of this analytical surface to describe the dynamics of this reaction, and reported four major drawbacks in this PES-2005 surface. First, the energy drop along the reaction path in the product valley does not reproduce ab initio calculations. Second, the surface neglects the FH···CH_3 van der Waals minimum in this product valley. Third, the PES-2005 shows much less FH(v') vibrational excitation than seen in experiments. Fourth, the FH(v') rotational distribution is considerably hotter than experiment.

In the present work, to correct the deficiencies of PES-2005, we report the construction of a new analytical potential energy surface for the title reaction, named PES-2006, and kinetics and dynamics calculations on it. Given that similar dynamics studies have been performed on different surfaces,[3,4] this is an interesting opportunity to analyze the role of the PES in the kinetic and dynamic description of this system. The article is structured as follows: In section II, previous high-level electronic structure calculations are reviewed to study energy and geometry aspects of this reaction, which are sensitive parameters in the calibration process. In section III, first, the development and calibration of the new PES-2006 is described and, second, a brief description of the other surfaces is given for comparison.[3,4] Section IV presents the computational details, and the new PES-2006 is tested against experimental and theoretical values used in the calibration in section V. The kinetics results using variational transition-state theory (VTST) are presented in section VI, while section VII presents a dynamics study using the QCT method. Finally, section VIII presents the conclusions.

II. Electronic Structure Calculations: A Review

Ab initio calculations have been reported by several laboratories[3−7] for the title reaction using very different levels (correlation energy + basis set). The main results are sum-

* Corresponding author. E-mail: joaquin@unex.es.

10.1021/jp0688759 CCC: $37.00
Published on Web 03/09/2007

TABLE 1: Theoretical Electronic Structure Calculations for the Saddle Point and Complexes (Energies in kcal mol^{-1} and Distances in Å)

method	ΔE	ΔV_a[a]	R(C−H′)	R(F−H′)	ref
	saddle point				
PMP4//UMP2/6-311+G(2d,p)	3.67	1.47	1.278	1.445	5
PMP4//UMP2/6-311+G(2df,2pd)	1.59	−0.13	1.120	1.458	5
QCISD(T)//QCISD/6-311+G(2d,p)	1.44	−0.36	1.124	1.515	5
QCISD(T)//QCISD/6-311+G(2df,2pd)	0.46	−0.65	1.113	1.551	5
QCISD(T)//QCISD/cc-pVDZ	4.40	1.70	1.160	1.376	3
QCISD(T)//QCISD/aug-cc-pVDZ	0.17	−1.08	1.127	1.586	3
MP-SAC2(F=0.78)	1.18	−0.10	1.124	1.564	3
CCSD(T)/aug-cc-pVTZ//MP2/aug-cc-pVDZ	−0.31	−2.29	1.137	1.466	4
CCSD(T)/aug-cc-pVTZ//CCSD(T)/aug-cc-pVDZ	0.40	−0.35	1.124	1.643	4
SRP-PM3/ROHF	0.82	−2.66	1.143	1.323	4
	reactant valley minimum				
QCISD/aug-cc-pVDZ	−0.33	−0.10			3
MP2/aug-cc-pVDZ	−0.23	−0.01			3
	product valley minimum[b]				
UMP2/6-311+G(2df,2pd)	−3.14	−1.37	2.137	0.984	5
QCISD/aug-cc-pVDZ	−2.28	−0.75	2.286	0.928	3
MP-SAC2			2.387	0.942	3
CCSD(T)/aug-cc-pVTZ	−2.62		2.2		4
SRP-PM3/ROHF	−3.79		1.8		4

[a] Enthalpy at 0 K (i.e., including the zero-point energy). [b] Energy values with respect to the products.

2marized in Table 1 for the saddle point and the complexes in the entry and exit channels.

We shall begin by analyzing the saddle point properties. Depending on the ab initio level used (correlation energy and basis set), the barrier height (ΔE) ranges from −0.31 to +3.67 kcal mol^{-1} and the adiabatic barrier (ΔV_a, i.e., when the zero-point energy is included) ranges from −2.66 to +1.70 kcal mol^{-1}. Given that there is no direct experimental measurement for comparison (some authors compare the barrier height with the experimental activation energy, which is only a coarse approximation), it is not at present possible to take any value as reference in the subsequent calibration process (see section III). At this point we can only say that when a better correlation energy is considered and larger basis sets are used, the barrier height (and the adiabatic barrier) is lower. Given that the reaction is very exothermic ($\Delta H_R = -32.0$ kcal mol^{-1}), the transition state is early; i.e., it appears soon in the reaction path. As a consequence, the transition state is "reactant-like", and the length of the C−H′ bond that is broken is similar to the case in methane, while the F−H′ bond formed is long. These distances also vary widely with the ab initio level used (Table 1).

With respect to the possible complexes, there is very little information about the possible complex in the entry channel.[3] The sparse theoretical information that is available indicates that this complex either will have a negligible influence or will not exist. There is somewhat more theoretical information about the possible complex in the exit channel. Depending on the level used, this complex is stabilized between 2.28 and 3.79 kcal mol^{-1} with respect to the products, and is about 1 kcal mol^{-1} more stable than the products when the zero-point energy is considered. As in the saddle point case, the C−H′ and F−H′ distances vary with the level used.

In spite of this wide range of values that is dependent on the level used, we conclude that the barrier height is very low, and that an FH···CH$_3$ complex exists in the exit channel, that is very little stabilized with respect to the products and is associated with the electric dipole moment−electric quadrupole moment interaction. These will be two theoretical criteria used in the calibration of our PES (see section III).

III. Potential Energy Surface

The title reaction consists of a hydrogen abstraction reaction from methane to yield the methyl radical, with a slow change in the geometry of the methyl group from pyramidal to planar along the reaction path. The functional form is the same as that of PES-2005,[2] and therefore will not be repeated here. Basically, it consists of a London−Eyring−Polanyi (LEP-type) function to describe the stretching modes, augmented by bending terms. It is important to note that this PES, as in the case of PES-2005, is symmetric with respect to the permutation of the four hydrogen atoms in methane, a feature especially interesting for dynamics calculations.

The main differences with respect to the earlier PES-2005 lie in the calibration process. The criterion chosen in the present study was broader than in previous work of our group.[2] As usual, we tried to reproduce the experimental variation of the forward rate constants with temperature in the experimentally measured range (180−410 K). However, the main innovation with respect to earlier surfaces is that we tried also to reproduce the topology of the reaction, from reactants to products, with special care taken in the reproduction of ab initio information along the reaction path and the investigation of complexes in the entry and exit channels. Therefore, in this paper we did not limit the calibration to the zone close to the saddle point.

Obviously, the complete construction of an analytical PES for polyatomic systems is not trivial and represents considerable computational and personal effort. In the present case 32 adjustable parameters were calibrated. Moreover, in this reaction there arise three further difficulties. First, given the very large exothermicity ($\Delta H_R = -32.0$ kcal mol^{-1}), the reaction path is very difficult to calculate because of a very flat PES in the entry channel. Second, in the experimental forward rate constants it is necessary to take into account the importance of the error bars. Persky[8] reported the expression $(1.28 \pm 0.15) \times 10^{-10}$ exp($-215 \pm 60/T$), cm^3 molecule^{-1} s^{-1}, over the temperature range 184−406 K, and Atkinson et al.[9] reviewed the existing information and reported the expression 1.3×10^{-10} exp($-215 \pm 200/T$) over the temperature range 180−410 K, with a larger error bar. For instance, at 300 K the rate constants

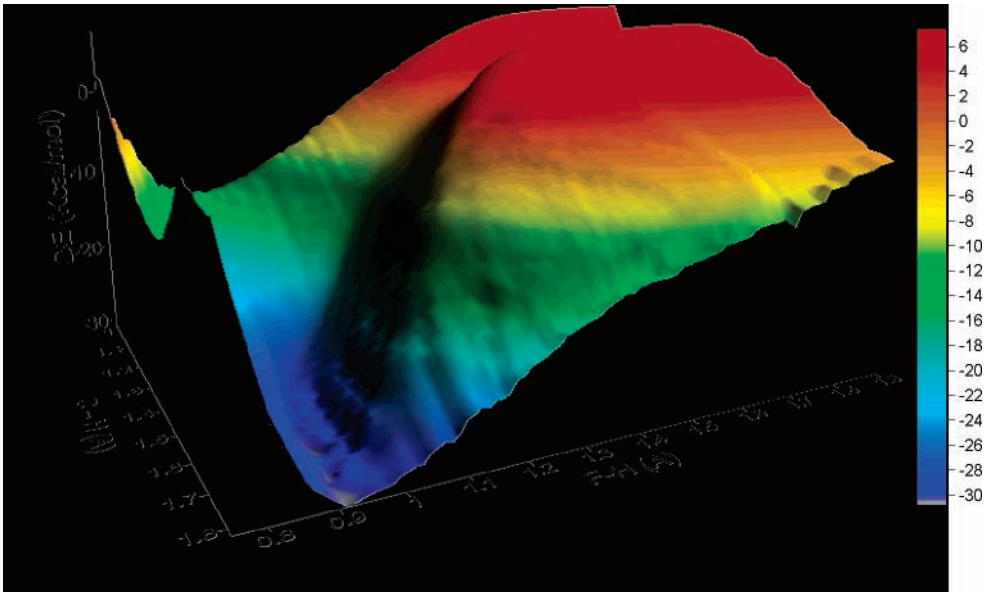

Figure 1. Three-dimensional representation of the potential energy surface for the gas-phase F(^{2}P) + CH_4 → FH + CH_3 reaction.

TABLE 2: Reactant and Product Properties[a] Calculated Using the Analytical Surface

	CH_4		CH_3		FH	
	PES-2006	expt[b]	PES-2006	expt[b]	PES-2006	expt[b]
			geometry			
R(C−H)	1.094	1.091	1.094	1.079		
R(F−H)					0.917	0.917
			frequency			
	3145	3018	3182	3184	4115	4139
	3145	3018	3182	3184		
	3145	3018	3072	3002		
	2984	2916	1380	1383		
	1538	1534	1380	1383		
	1538	1534	580	580		
	1344	1306				
	1344	1306				
	1344	1306				
			energy			
ΔH_r[c]	−32.00	−32.00				
ZPE	27.92	27.10	18.27	18.18	5.88	5.92

[a] Distances in Å, frequencies in cm^{-1}, energies in kcal mol^{-1}. [b] Experimental data from ref 20. [c] Enthalpy of reaction at 0 K.

range from 3.25×10^{-10} to 12.3×10^{-11}, with a recommended value of 6.35×10^{-11} cm^3 $molecule^{-1}$ s^{-1}, close to the recommended value of Persky. Third, the F atom presents two spin−orbit electronic states, $^2P_{3/2}$ and $^2P_{1/2}$, which are split by only 404 cm^{-1} (1.15 kcal mol^{-1}). A priori, there is the possibility of reaction from these two states. Unfortunately, there are no relativistic theoretical studies of this reaction, and a study of this type is beyond the scope of the present work. Therefore, we shall take the similar and very well studied F($^2P_{3/2}$ and $^2P_{1/2}$) + H_2 atom−diatom reaction for comparison purposes. Alexander et al.[10] found, first, that reactivity of the excited spin−orbit state of F is small, 10−25% of the reactivity of the ground spin−orbit state and, second, that the overall dynamics of the F + H_2 reaction will be well described by calculations on a single, electronically adiabatic PES. We assume this same behavior for the similar F + CH_4 reaction.

The final functional form and the adjustable parameters for the new PES-2006 surface are given on our Web page,[11] and a three-dimensional (3D) representation is shown in Figure 1. Note that this surface is semiempirical, in the sense that both experimental and theoretical information are used to calibrate it.

Before finishing this section, and given that comparison with another two recent full surfaces will be carried out in this paper, we shall briefly describe these surfaces, referring readers to the original papers for more details. Castillo et al.[3] constructed their PES based on 1100 points calculated at the MP2-aug-cc-pVDZ level (energy, gradient, and Hessian) and subsequent scaling using the SAC method of Truhlar et al.[12] Then these points were interpolated using Collins's method.[13] Thus, this surface is an interpolated ab initio PES. The barrier height is low, 1.18 kcal mol^{-1} (−0.10 when the ZPE is included), but the reaction exothermicity, −40.91 kcal mol^{-1}, is very far from the experimental value, −32.0 kcal mol^{-1}. As was noted by the authors, better agreement with experiment is only possible when high-level ab initio calculations are used, but then the computational cost is very high. To avoid this problem, Troya[4] constructed a surface for the title reaction using the specific-reaction parameter (SRP) Hamiltonian method based on parameter-model-3 (PM3) semiempirical calculations. The barrier height is lower than that above, but above all the vibrationally adiabatic barrier, −2.66 kcal mol^{-1}, is especially low compared with other ab initio calculations (Table 1). In these two surfaces, no kinetics studies were carried out, only dynamics studies using

TABLE 3: Saddle Point Properties,[a] Using Different PES and ab Initio Calculations

	PES-2006	PES-2005[b]	QCI[c]	CC[d]	MP-SAC2[e]
			geometry		
R(C−H)	1.094	1.094	1.085	1.101	1.099
R(C−H′)	1.100	1.107	1.114	1.124	1.124
R(F−H′)	1.777	1.550	1.551	1.643	1.564
			frequency		
	3133	3127	3201	3168	3220
	3133	3127	3201	3161	3220
	3058	3032	3094	3057	3084
	2880	2711	2389	2606	2486
	1485	1416	1513	1486	1458
	1485	1416	1513	1472	1458
	1283	1221	1298	1298	1231
	1265	1201	1298	1276	1231
	1265	1201	1297	1231	1231
	122	119	116	109	85
	122	119	116	86	85
	122i	106i	283i	270i	327i
			energy		
$\Delta E^{\ddagger}$	0.35	0.25	0.46	0.40	1.18
$\Delta H^{\ddagger}$(0 K)	−0.07	−0.45	−0.65	−0.35	−0.10
ZPE	27.50	26.72	27.21		

[a] Distances in Å, frequencies in cm^{-1}, energies in kcal mol^{-1}. C_{3v} symmetry. [b] Surface from our previous work.[2] [c] QCISD(T)//QCI/6-311+G(2df,2dp) from ref 5. [d] CCSD(T)/aug-cc-pVTZ/CCSD(T)/aug-cc-pVDZ from ref 4. [e] MP2/aug-cc-pVDZ with SAC correction ($F = 0.78$) from ref 3.

TABLE 4: Forward Thermal Rate Constants for the F + CH_4 Reaction[a]

T (K)	PES-2006	PES-2005[b]	expt[c]
180	4.55	3.59	3.9
200	4.83	3.97	4.4
225	5.14	4.41	5.0
250	5.48	4.82	5.5
275	5.78	5.16	6.0
298	6.05	5.49	6.3
300	6.07	5.51	6.4
325	6.36	5.88	6.7
350	6.65	6.21	7.0
400	7.22	6.82	7.6
500	8.36	8.00	

[a] ICVT rate constants, in 10^{-11} cm^3 molecule^{-1} s^{-1}. [b] ICVT rate constants from ref 2. [c] Experimental values from ref 8.

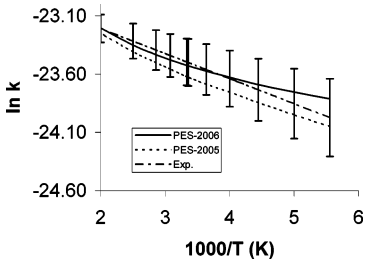

Figure 2. Arrhenius plots of ln k (cm^3 molecule^{-1} s^{-1}) for the forward thermal rate constants against the reciprocal of temperature (K) in the range 180−500 K. Solid and dashed lines: our VTST values for the PES-2006 and PES-2005 surfaces, respectively. Experimental values (from ref 8): dashed−dotted line, including the error bars.

quasi-classical trajectory (QCT) calculations, although with different code programs, VENUS96 in the first case and the direct reaction coordinate (DRC) facility of the GAMESS code in the second.

IV. Computational Details

In the kinetics study, we used the variational transition-state theory (VTST).[14] Starting from the saddle point geometry, we followed the reaction path toward both reactants and product, obtaining the minimum energy path, MEP,[15] in the range $s = \pm 3.0$ bohr; s is the reaction coordinate. Along the MEP, we calculated vibrational frequencies after projecting out the motion along the reaction path using redundant internal coordinates.[16,17] With this information, we calculated the ground-state vibrationally adiabatic potential curve

$$V_a^G(s) = V_{MEP}(s) + \epsilon_{int}^G(s) \quad (1)$$

where $V_{MEP}(s)$ is the classical energy along the MEP with its zero of energy at the reactants and $\epsilon_{int}^G(s)$ is the zero-point energy at s. Rate constants were estimated by using improved canonical variational transition-state theory (ICVT).[14,18] Quantum effects in motions transversal to the reaction path were included by using quantum-mechanical vibrational partition functions in the harmonic approach, while we found those quantum effects in the motion along the reaction path to be negligible due to the very flatness of the topology. All kinetics calculations were performed using the general polyatomic rate constants code POLYRATE.[19] In the present work we included the $^2P_{1/2}$ excited state of F (with an excitation energy[20] of 404 cm^{-1}) in the reactant electronic partition function, while the rotational partition functions were calculated classically.

In the dynamics study we performed quasi-classical trajectory (QCT) calculations[21−23] using the VENUS96 code,[24] customized to incorporate our analytical PESs. It was also modified to compute the vibrational energy in each normal mode to obtain information on the CH_3 product vibrational distribution in the exit channel. Since VENUS freely rotates the molecules along the trajectories, the normal mode energy calculation is preceded by a rotation of the molecule in order to maintain the orientation of the optimized geometry of the methane molecule for which the normal-mode analysis was performed. Once this is done, a projection of the displacement and momentum matrices on the normal-mode space allows one to compute the potential and kinetic energy for each normal mode. The energy in each harmonic normal mode was computed for the last geometry (coordinates and momenta) on the reactive trajectories. This approach had been used in an earlier paper by our group[25] with excellent results.

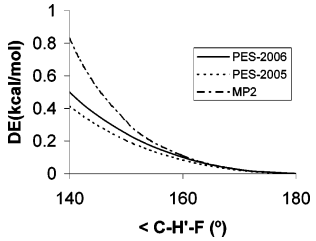

Figure 3. Saddle point bending energy curves (C−H′−F) for the F + CH_4 reaction. The remaining internal coordinates have been kept fixed for the respective methods. Solid and dashed lines: our values for the PES-2006 and PES-2005 surfaces, respectively. Dashed−dotted line: MP2/6-311G(d,p) ab initio calculations. Note that the 180° value corresponds to the saddle point.

The accuracy of the trajectory was checked by the conservation of total energy and total angular momentum. The integration step was 0.01 fs, with an initial separation between the F atom and the methane center of mass of 6.0 Å, and a maximum value of the impact parameter of 3.5 Å. To simulate the experimental conditions, we considered a relative translational energy of 1.8 kcal mol^{-1} and a methane rotational energy of 20 K. Batches of 100 000 trajectories were calculated, where the impact parameter, *b*, was sampled by

$$b = b_{\max} R^{1/2} \tag{2}$$

where *R* is a random number in the interval [0,1].

A serious drawback of the QCT calculations is related to the question of how to handle the quantum-mechanical zero-point energy (ZPE) problem in the classical mechanics simulation.[26−35] Many strategies have been proposed to correct for this quantum-dynamics effect (see, for instance, refs 26−30 and 33, and references therein), but no completely satisfactory alternatives have emerged. Here, we employed a pragmatic solution, the so-called passive method,[30] consisting of discarding all the reactive trajectories that lead to either an FH or a CH_3 product with a vibrational energy below their respective ZPEs. This we call histogram binning with double ZPE correction (HB-DZPE).

V. Test of Consistency of the New PES. Calibration and Comparison with ab Initio Calculations

Before beginning the analysis of the kinetics and dynamics results obtained using the PES-2006 now constructed, a consistency test of the calibration was performed. Because both theoretical and experimental information were used in this process, this analysis simply informs one of the consistency of the parametrization.

(i) The results of the final fit are listed in Table 2 for reactants and products, and in Table 3 for the saddle point. In general, the reactant and product properties agree very well with the experimental data,[20] with the most significant difference being 0.02 Å for the C−H bond length in the methyl radical. With respect to the vibrational frequencies, the small differences found balance out between reactants and products, yielding an enthalpy of reaction at 0 K of −32.0 kcal mol^{-1}, in close agreement with the experimental value.[20]

While no complex was found in the entry channel, in the exit channel we found one van der Waals complex, stabilized by 1.0 kcal mol^{-1} with respect to the products and a C−H′ bond length of 2.000 Å (F−H′ = 0.918 Å). Undoubtedly this very flat complex obtained with our PES will have little or no influence on the kinetics, but it may affect the rotational excitation of the FH product.

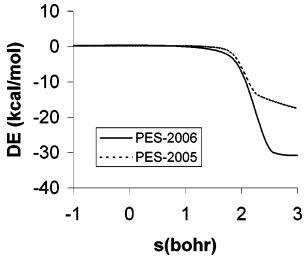

Figure 4. Minimum energy paths (MEPs) for the PES-2006 (solid line) and PES-2005 (dashed line) surfaces.

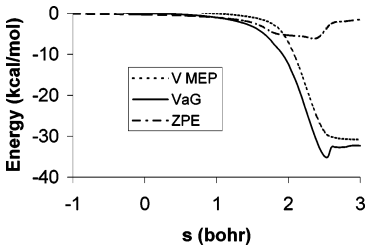

Figure 5. Classical potential energy curve, V_{MEP}, zero-point energy, ΔZPE, and vibrationally adiabatic potential energy curve, ΔV_a^G, as a function of the reaction coordinate, *s*. All quantities are with respect to the reactants.

With respect to the saddle point geometry, in general the ab initio information[3−7] was reasonably well reproduced, with the most significant differences being a longer F−H′ bond (H′ being the abstracted hydrogen). In general, the ab initio data show that the F−H′ bond is longer than the C−H′ bond. This tendency is reproduced in this new PES-2006. At the saddle point the length of the bond that is broken (C−H′) increases by only 1%, and the length of the bond that is formed (F−H′) is 94% larger than at the products. This indicates that the reaction of the F atom with methane proceeds via a "very early" transition state; i.e., it is a reactant-like transition state. This is the expected behavior that would follow from the large exothermicity of the reaction. This saddle point is well characterized by one imaginary frequency.

More interesting is the barrier height comparison (Table 3). In section II, we analyzed different theoretical levels, concluding that the classical barrier height is very sensitive to the extension of the one-electron basis set, a general problem in computational chemistry. Although the range of values of the barrier height (Table 1) is wide, one observes that the value decreases as the level of calculation increases. The barrier height obtained with our PES-2006, 0.35 kcal mol^{-1}, agrees with this tendency, and one can consider this value as reasonable.

It should be borne in mind that the agreement in geometry, vibrational frequencies, and energy, for reactants, products, intermediate complexes, and saddle point, is a consequence of the fitting procedure used, and simply represents a check of the consistency of the parametrization.

The above discussion about the barrier height, a single point on the whole surface, reflects the need for very high level ab initio calculations to correctly describe a reactive system. Given that thousands of calculations are necessary to perform the kinetics and dynamics calculations, this is even today a prohibitive task in polyatomic systems, and the problem increases with molecular size. In view of this very demanding process, which usually requires a final ad hoc refit, the alternative of obtaining a global PES such as the one developed in the present work becomes essential for accurate kinetics and dynamics studies.

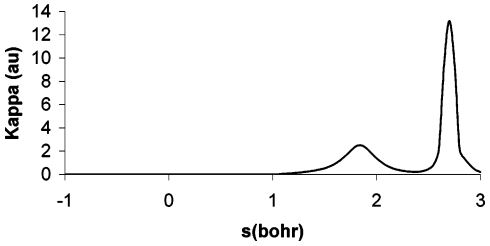

Figure 6. Reaction path curvature, κ, as a function of reaction coordinate, s.

(ii) Another important test of consistency is the comparison with the experimental rate constants which were used in the calibration process. Table 4 lists the variational ICVT thermal forward rate constants obtained with this PES-2006, together with the experimental and our previous PES-2005 rate constants for the temperature range 180−500 K. Figure 2 shows the corresponding Arrhenius plot. The new parametrization of the surface, PES-2006, reproduces the experimental data in the common temperature range, taking into account the experimental error bar. Since the experimental thermal forward rate constants were used in the calibration process, again this represents simply another check on the consistency of the parametrization.

To provide the most appropriate comparison with experiment, the phenomenological activation energy was computed as the local slope of the Arrhenius plot. Over the common temperature range, 180−410 K, our theoretical result, 0.32 kcal mol^{-1}, agrees closely with that from experiment,[8] 0.43 ± 0.12 kcal mol^{-1}.

(iii) To confirm the accuracy and behavior of our analytical PES, we compared it against ab initio calculations in sensitive zones of the reaction such as the bending of the linear approach and the potential energy curve. It is well-known that there is a correlation between the bending frequency of the collinear saddle point (C−H′−F) and the product F−H′ rotational distribution. Schatz et al.[36,37] found that surfaces having the same saddle point but differing dependence of energy on the bending angle showed very different rotational excitation in the products, concluding that looser saddle points imply hotter rotations. To test this energy dependence of the C−H′−F bending angle, we compared the values from our analytical PES and our previous PES-2005 with ab initio calculations at the MP2=FULL/6-311G(d,p) level (Figure 3). Although the energy variation was practically isotropic in the wide range 140°−180°, with variations of only 0.5 kcal mol^{-1}, the new PES-2006 is slightly more repulsive than PES-2005, and closer to the ab initio values. A priori, this represents a rotationally colder product, one of the goals of the present work.

Moreover, this isotropic behavior would explain two interesting features of this reaction. First, there is the strong dependency of the level of calculation on the C−H′−F angle at the saddle point. Thus, we performed MP2=FULL ab initio calculations using three different and modest basis sets: 6-31G, 6-31G(d,p), and 6-311G(d,p). While in the first and third cases we found a collinear saddle point, $\theta = 180°$, the 6-31G(d,p) basis set yielded a bent geometry, $\theta = 158.6°$. In these three cases, we confirmed that the stationary point is a true saddle point, characterized by one and only one imaginary frequency. Castillo et al.,[3] Troya,[4] and Roberto-Neto et al.[7] found similar behavior using the same basis set, aug-cc-pVDZ, but different correlation energy methods: MP2, QCISD, and CCSD(T). While the first two levels yield a collinear geometry, the third yields a bent geometry, $\theta = 153.4°$. Second, there is the experimental finding that the FH product rotational distribution is hotter than the corresponding distribution of the diatomic product in analogous hydrogen abstraction reactions, such as H + CH_4, Cl + CH_4, and O(^{3}P) + CH_4. These two features were also found in the results of Castillo et al.[3] and Troya[4] using their interpolated ab initio and SRP-PM3 surfaces, respectively. This all would seem to lend confidence to the surface constructed in the present paper.

With respect to the potential energy curve, Kuntz et al.[38] noted that for exothermic triatomic systems the release of energy into vibration depends on the location of the region of the PES responsible for the product repulsion. Figure 4 shows the potential energy curve using the new PES-2006, and for comparison the previous PES-2005. Troya[4] noted that one of the deficiencies of our previous PES-2005 surface was that the region of product repulsion occurs more toward the products than predicted by ab initio calculations. Clearly, the new PES-2006 corrects this deficiency, which will represent a larger release of energy into vibration, another goal of the present work. This can be seen in more detail if we compare our Figure 4 with Figure 3 in Troya's paper. Finally, it again needs to be borne in mind that, as the bending curve and the potential energy curve were used in the calibration process, this represents simply another check of the consistency of the parametrization.

In sum, therefore, the present work involved the calibration of the surface, taking into account close and far zones relative to the saddle point, i.e., considering the topology of the complete reactive system from reactants to products, with special attention paid to the possible reactant or product complexes. This represents an innovation with respect to previous work of our group.

VI. Kinetics Results and Discussion

VI.1. Reaction Path and Coupling Terms. For the PES-2006 surface, Figure 5 shows the classical potential energy, V_{MEP}, the ground-state vibrationally adiabatic potential energy curve, ΔV_a^G, and the change in the local zero-point energy, ΔZPE, as a function of s over the range −1.0 to +3.0 bohr. Note that ΔV_a^G and ΔZPE are defined as the difference between V_a^G at s or ZPE at s and their values for reactants.

The ΔZPE curve drops at about $s = +2.0$ bohr and shows a broad well. This behavior is typical of hydrogen abstraction reactions, and the change with s is mainly due to the drop in the CH_4 stretching corresponding to the normal mode breaking during the reaction, which evolves to the FH stretching mode forming in the product (reactive mode). As a consequence, the ΔV_a^G curve presents a well, stabilized 3.03 kcal mol^{-1} with respect to the products. It is located at $s = +2.55$ bohr in the product channel, and represents the following geometry: F−H′ = 1.173 Å and C−H′ = 1.382 Å.

Two important features are necessary to note. First, this well does not correspond to the van der Waals complex found in the product channel, which appears at a larger C−H′ distance: 2.000 Å (F−H′ = 0.918 Å). Second, this mechanism that assumes the presence of a quasi-bound complex does not exclude the possibility of a direct mechanism: due to the very large exothermicity of the reaction, the system has enough energy to go through the well without falling into it. Thus, the two mechanisms take place simultaneously, and the overall dynamics of the system is the sum of the two mechanisms. Obviously, this simultaneity will be a problem in the experimental detection of this quasi-bound complex.

Along the MEP the coupling terms, $B_{k,F}(s)$, measure the coupling between the reaction coordinate (F) and the orthogonal bound modes (k). These coupling terms are the components of

TABLE 5: Kinetic Isotope Effects for F + CH_4/F + CD_4 as a Function of Temperature

T (K)	PES-2006	PES-2005	expt	expt[a]
180	1.85	2.07		1.72 ± 0.05
200	1.79	2.01		1.63 ± 0.05
225	1.72	1.94		1.54 ± 0.05
250	1.68	1.87		1.48 ± 0.05
283	1.61	1.79	1.9 ± 0.9,[b] 1.7 ± 0.3[c]	1.41 ± 0.05
298	1.59	1.77	1.4 ± 0.1,[d] 1.5 ± 0.5[e]	1.38 ± 0.05
300	1.59	1.76		
325	1.55	1.73		
350	1.53	1.70		
400	1.48	1.63		
500	1.40	1.54		

[a] Reference 47; $k(F+CH_4)/k(F+CD_4) = (0.99 \pm 0.02)\exp(100 \pm 5/T)$. [b] Reference 44. [c] Reference 45. [d] Reference 42f. [e] Reference 46.

TABLE 6: Kinetic Isotope Effects for F + $HCHD_2$/F + $DCDH_2$ as a Function of Temperature

T (K)	PES-2006	expt[a]
180	1.34	1.72
200	1.32	1.61
225	1.30	1.50
250	1.28	1.41
298	1.26	1.30
300	1.26	
325	1.24	
350	1.23	
400	1.22	
500	1.19	

[a] Reference 48; $k(F+HCHD_2)/k(F+DCDH_2) = (0.81 \pm 0.03)\exp(138 \pm 7/T)$, for 159−298 K.

the reaction path curvature, $\kappa(s)$, defined as

$$\kappa(s) = \{\sum [B_{k,F}(s)]^2\}^{1/2} \quad (3)$$

and control the nonadiabatic flow of energy between these modes and the reaction coordinate.[39−41] They will allow us to give a qualitative explanation of the possible excitation of reactants and/or products, i.e., dynamic features, which are another sensitive test of the new surface. Figure 6 shows the curvature of the reaction path as a function of s. This figure shows the same behavior as reported with PES-2005, and its discussion will not be repeated here. We would only note that the lowest peak ($s = +1.85$ bohr) is due to the strong coupling of the reaction path to the CH_3 umbrella bending mode, while the highest peak ($s = +2.70$ bohr) is due to the coupling of the reaction path to the F−H stretch mode. Therefore, for thermal reactions these two modes will appear vibrationally excited. Moreover, while the latter mode needs too much energy to be excited by translational to vibrational energy transfer, the former mode is a good candidate to receive this energy during the time that the quasi-bound complex exists. These qualitative results agree with our previous PES-2005 and with experiments,[42,43] and will be analyzed in more detail below in the dynamics study.

VI.2. Kinetic Isotope Effects. It is well-known that the KIEs provide a very sensitive test of several features of the shape of the new surface (barrier height and width, and zero-point energy near the dynamic bottleneck). This magnitude is defined following the convention that the rate for the lighter isotope is always in the numerator. Hence, a value greater than 1 is considered a "normal" KIE, while a value less than 1 is an "inverse" KIE. Two sets of KIEs (one more than in our previous PES-2005 study) were calculated on this surface (Tables 5 and 6) for the temperature range 180−500 K, and compared with the available experimental values. The F + CH_4/F + CD_4 KIEs are listed in Table 5 together with the sparse experimental values for comparison.[42f,44−47] The KIEs obtained with the PES-2006 surface agree reasonably well with the corresponding common experimental data at 283 and 298 K, taking into account the large uncertainties of the experimental values. Recently, Persky[47] has reported the KIEs as a function of temperature over the temperature range 183−298 K. Our PES-2006 reproduces the tendency found experimentally, and although they are slightly greater, they improve the results from our previous PES-2005.

We also calculated the F + $HCHD_2$/F + $DCDH_2$ KIEs (Table 6) and compared them with the only (and now rather old) experimental measurement[48]

$$F + HCHD_2 \rightarrow FH + CHD_2$$

$$F + DCH_2D \rightarrow FD + CH_2D$$

In the common temperature range, the PES-2006 reproduces the variation with temperature. Although our values are somewhat smaller than experiment, the agreement at 298 K is excellent.

Before finishing this kinetics section, it is interesting to note that this analysis, although of macroscopic properties, is very interesting for defining the accuracy of the new PES. It is usually absent from other studies, for example in the two surfaces recently developed by other groups.[3,4]

VII. Dynamics Results and Discussion

VII.1. Product Energy Partition. Although there is no direct experimental measurement of this dynamics property, Zhou et al.[49] reviewed the earlier experimental information and found that the energy partitioning can be summarized as follows: fv(FH), 0.61; fr(FH), 0.03; fv(CH_3), 0.03; fr(CH_3), 0.02; and ft, 0.31; i.e., the energy is released mainly as vibration in the FH product and relative translation of products, with negligible internal energy in the CH_3 coproduct.

The QCT results on our PES-2006 are listed in Table 7 together with the experimental estimate[49] and other QCT results on different PESs.[2−5,50] First, the PES-2006 results have remarkably improved the partition energy distribution obtained with our previous PES-2005, one of the main goals in the present work. Second, in general, all QCT calculations on different surfaces agree poorly with experiment, with overestimates of the CH_3 internal energy (except the Kornweitz et al. calculation) and underestimates of the relative translational energy. Given that very different potential energy surfaces are used, these differences may be due to limitations of the QCT method in describing this system, and/or to different treatments of the zero-point energy problem. Obviously, intrinsic deficiencies of the different surfaces cannot be discarded.

To test the influence of the zero-point energy correction on this property, we also performed calculations considering all trajectories, i.e., without removing the trajectories with energies

TABLE 7: Product Energy Partition at 1.8 kcal mol^{-1} Collision Energy

	PES-2006	expt[a]	PES-2005[b]	KPL[c]	CABMFV[d]	Troya[e]
fv(FH)	0.66	0.61	0.40	0.75	0.53	0.67
fr(FH)	0.10	0.03	0.16	0.15	0.07	0.04
fv(CH_3)	0.11	0.03	0.27	~0	0.27	0.14[f]
fr(CH_3)	0.04	0.02	0.02	~0	0.03	
ft	0.09	0.31	0.14	0.10	0.10	0.15

[a] Reference 49. [b] LEPS-type PES from ref 2. [c] LEPS-type PES from ref 50. [d] Interpolated ab initio PES at the MP-SAC2 level from ref 3. [e] Semiempirical SRP-PM3 PES from ref 4. [f] This value corresponds to the internal energy of the CH_3.

TABLE 8: FH(v') Vibrational Populations at 1.8 kcal mol^{-1} Collision Energy

reference	$v' = 0$	$v' = 1$	$v' = 2$	$v' = 3$
this work	0.01	0.15	0.82	0.02
expt[a]	0.04 ± 0.04	0.19 ± 0.03	0.67 ± 0.02	0.11 ± 0.01
KPL[b]	0.03	0.10	0.54	0.33
TMBC[c]	0.0	0.10	0.72	0.18
CABMFV[d]	0.20	0.23	0.29	0.22
T[e]	0.0	0.21	0.67	0.13
PES-2005[f]	0.08	0.63	0.28	0.01

[a] Reference 42g. [b] LEPS-type PES from ref 50. [c] Ab initio triatomic analytical representation from ref 5. [d] Interpolated ab initio PES at the MP-SAC2 level from ref 3 [e] Semiempirical SRP-PM3 PES from ref 4 [f] LEPS-type PES from ref 2.

below the ZPE of the products. The energy partition is as follows: fv(FH), 0.53; fr(FH), 0.08; fv(CH_3), 0.30; fr(CH_3), 0.03; and ft, 0.06. Thus, the agreement with experiment is poorer: the FH vibrational energy diminishes, while the CH_3 vibrational energy increases. Therefore, the results are very sensitive to the ZPE criterion chosen.

VII.2. Excitation Function. The excitation function (reaction cross section versus collision energy) was measured experimentally by Shiu et al.[51] for the energy range 0.48−7.3 kcal mol^{-1} for the formation of the ground state CH_3 ($v = 0$). This function shows a steep increase from the threshold up to a collision energy of ≈2 kcal mol^{-1}, and then decays as the collision energy increases. This behavior differs notably from those for the analogous F + H_2 reaction,[10b,52,53] and also for the isotopic F + CD_4 reaction.[49]

Previous QCT calculations on interpolated ab initio,[3] semiempirical SRP-PM3,[4] and analytical LEPS-type (PES-2005)[2] surfaces found a rapid increase from the threshold up to a peak, in accordance with experiment, but then a gradual decrease as the energy increases, in contrast with experiment. Therefore, those previous surfaces do not reproduce the whole experimental behavior. It is interesting to note the very strange behavior obtained by Troya[4] using our previous PES-2005 surface (see Figure 6b in the original paper), which strongly contrasts with that obtained by Castillo et al.[3] and the present work using the same surface. It is not yet clear what the reason is for this major discrepancy, but we would note that different programs were used for the QCT calculations: the DRC facility of GAMESS in Troya's study and the VENUS96 code in the other two.

Neither do QCT calculations on the present PES-2006 reproduce the experimental behavior, and the excitation function presents an oscillatory pattern in the region around 2 kcal mol^{-1} (Figure 7). In analyzing this behavior in more detail, we first observed that the falls at 2.5 and 3.5 kcal mol^{-1} are because in many trajectories the FH product is moving away and approaching the CH_3 coproduct for a very long period of time, producing a quasi-trapped resonance state. This means that many trajectories are not reactive at these energies, and is a signature similar to that of a reactive resonance. Indeed, these reactive resonances have recently been reported experimentally[54] and theoretically[55,56] for the title reaction.

Second, in considering the vibrational-state contribution to this function (Figure 7), we found that the oscillatory pattern

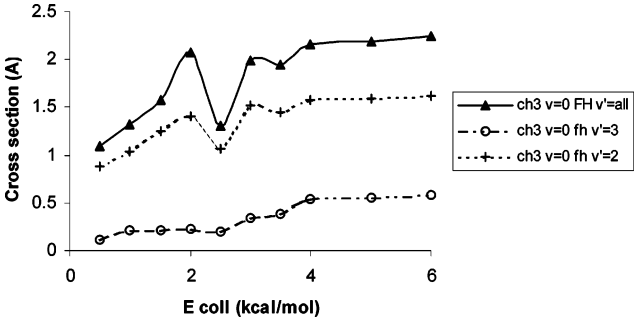

Figure 7. Excitation function for the F + CH_4 → FH(v') + CH_3(v'=0) reaction using the PES-2006 surface. The solid line includes all FH vibrational states. Dashed line and cross symbols, FH(v'=2) level; dashed−dotted line and circle symbols, FH(v'=3) level.

of the complete function is mainly due to the FH(v'=2) state, while the FH(v'=3) state shows a smoother behavior, although it also presents a step character.

Two final considerations need to be made. First, an oscillatory pattern is not always related to resonance behavior, and second, although the quasi-bound state is observed in the QCT calculations, these QCT results need to be taken with extreme caution because of their classical nature, and obviously a firmer conclusion about this resonance would only be possible using quantum-mechanical (QM) calculations, which is beyond the scope of this study.

VII.3. FH(v',j') Product Rovibrational Distribution. The FH(v') vibrational distributions calculated with the QCT method using different surfaces are listed in Table 8, together with the available experimental data for comparison.[42g]

Except on the PES-2005 surface and the interpolated ab initio PES,[3] all the QCT calculations reproduce the experimental behavior, where vibrational population inversion is found, with a peak in $v' = 2$. In agreement with the goals set out in the Introduction, the PES-2006 improves the results of the earlier PES-2005, since it reproduces the ab initio reaction path better (Figure 4), making a deeper fall in energy in the product valley, in agreement with ab initio calculations.

The QCT vibrationally state resolved FH(v') rotational distributions using the PES-2006 are plotted in Figure 8, together with the QCT results on our previous PES-2005 and experimental values.[42g] The PES-2006 reproduces the experimental tendency, i.e., when the vibrational state is higher, the rotational

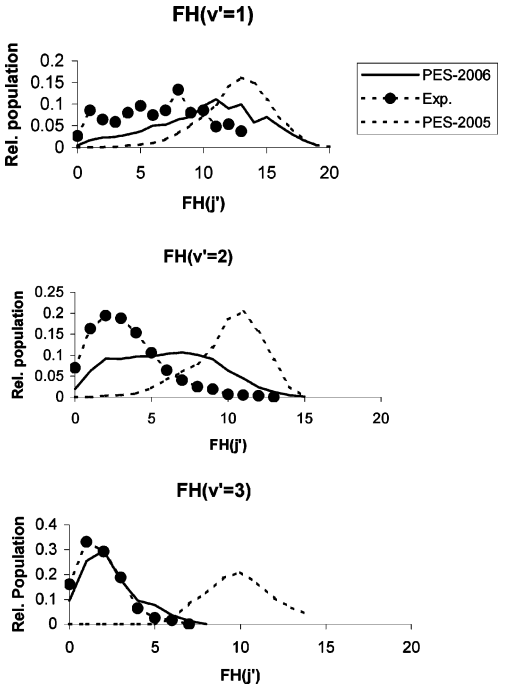

Figure 8. Rotational populations for F + CH_4 → FH(v',j') + CH_3 reaction. The distributions are normalized so that the area under the common levels is the same. The solid line corresponds to the results with the PES-2006 surface, and the dashed line corresponds to the experimental values from ref 42g.

TABLE 9: Percentage Population of CH_3 Coproduct Vibrational States[a]

CH_3 vibrational state[b]		
		population
ν_2'	0	40
	1	30
	2	30
ν_4'	0	70
	1	24
	2	6
ν_1'	0	89
	1	9
	2	1
ν_3'	0	96
	1	4
	2	0

[a] Ground-state methane reactant, at 1.8 kcal mol^{-1}. [b] ν_2', umbrella bending, 580 cm^{-1}; ν_4', deformation bending, 1380 cm^{-1}; ν_1', symmetric stretch, 3072 cm^{-1}; ν_3', asymmetric stretch, 3182 cm^{-1}.

distribution is colder, although our theoretical values are hotter by 1−2 values of j' and broader. It is interesting to note the marked improvement with respect to the previous PES-2005 results for all FH(v') states, especially for the FH(v'=3) state, where the j' maximum passes from j' = 10 to j' = 2, at only one value from experiment. Obviously, this behavior is related to the more repulsive bending curve of the PES-2006 surface (Figure 3), and the lower average rotational fraction, ⟨fr(FH)⟩ = 0.10 versus 0.16 for the PES-2005 surface (Table 7). The other surfaces, interpolated ab initio[3] and semiempirical SRP-PM3,[4] also present differences with respect to experiment, indicating that this property is strongly dependent on the construction of the surface, and/or the different treatment of the ZPE problem.

VII.4. CH_3(v') Coproduct Vibrational Distribution. Table 9 lists the percentage vibrational excitation of the CH_3 coproduct for the ground-state methane and a collision energy of 1.8 kcal mol^{-1}. The ground-state vibrational methane gives mainly ground-state CH_3 products. The percentage diminishes with the modes: 60% with excited umbrella bending (ν_2'), 30% with excited deformation bending (ν_4'), and between 10 and 4% in stretching excited modes. These results agree with the experimental evidence,[43] and confirm the purely qualitative description obtained previously with the analysis of the kappa factors (section VI.1).

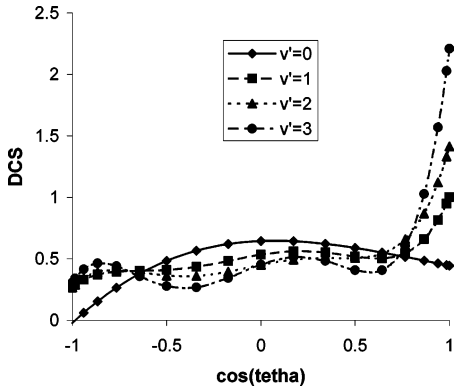

Figure 9. Product angular distribution for the F + CH_4 → FH(v') + CH_3 reaction, for different vibrational FH states.

VII.5. Differential Cross Section. The differential scattering dynamics of the title reaction was determined experimentally by Harper et al.[57] via high-resolution IR laser dopplerimetry. Although there are experimental difficulties and the results are limited in angular resolution, the authors find for the FH(v'=1) and FH(v'=2) states a clear propensity for forward/backward, $|\cos(\theta)| \approx 1$, versus sideways scattering, $|\cos(\theta)| \approx 0$, although unfortunately the forward versus backward scattering cannot be well characterized.

The QCT vibrationally state resolved FH(v') scattering angular distributions on PES-2006 at collision energy of 1.8 kcal mol^{-1} are plotted in Figure 9. While for the FH(v'=0) state the sideways distribution dominates the forward/backward, for the all other FH(v'=1,2,3) states the forward/backward scattering dominates the sideways, in agreement with experiment. Moreover, as the vibrational state increases, FH(v'=1 → v'=3), the scattering becames increasingly forward shaped. This result for the FH(v'=3) state agrees with the experimental data for the analogous F + H_2 → FH (v'=3) + H reaction,[58] and with the behavior of the title reaction at high impact parameters, called peripheral reactions by Kornweitz et al.[50]

Comparing these results with previous QCT calculations on different surfaces, ones observes that the earlier PES-2005 surface presented a similar behavior, the forward scattering increasing with the vibrational state, while the interpolated ab initio surface by Castillo et al.[3] obtained scattering that was predominantly backward at any FH(v') state. Troya,[4] using the semiempiral SRP-PM3 surface, only reported results for all the FH(v') vibrational states, without differentiating vibrational levels.

To shed more light on this problem, we analyzed the evolution of the angular distribution as a function of the collision energy. Because of the statistics, Figure 10 shows the 3D plot of the differential cross section (DCS)−collision energy (Ecoll)−θ for the most populated FH(v'=2) state. One observes a notable change of DCS with collision energy. At low energies, the DCS is practically sideways, but as the energy increases forward scattering predominates, with sudden changes at energies of 2.5 and 3.5 kcal mol^{-1}. This pattern is reminiscent of the resonance signatures observed for the atom−diatom F + HD → FH + D

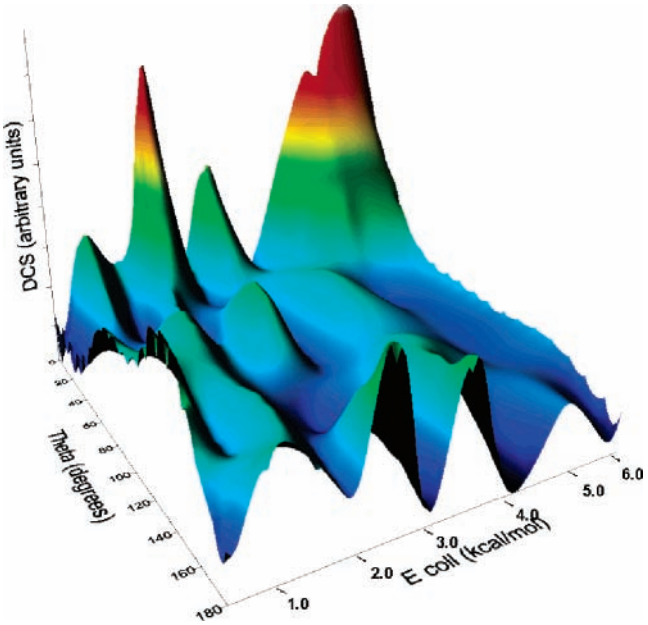

Figure 10. Three-dimensional representation of the evolution of the differential cross section as a function of the collision energy in the range 0.5−6.0 kcal mol^{-1}.

reaction,[59] and the polyatomic Cl + CH_4 → ClH + CH_3 reaction,[60] and could explain the experimental resonance reported by Shiu et al. for this reaction.[54] These authors suggest that the mechanism for this possible resonance is a Feshbasch resonance due to dynamic trapping in wells on the vibrationally adiabatic PES. As noted in section VI.1, in the present study using the PES-2006 surface we found a deep well on the vibrationally adiabatic curve, and we suggest that this resonance is assigned to the CH_3 bending umbrella mode.

VIII. Conclusions

In this work we have recalibrated a previous analytical potential energy surface for the gas-phase F(^{2}P) + CH_4 → FH(v',j') + CH_3(v') reaction. The new surface, named PES-2006, is also semiempirical, the innovation being an extension of the calibration criteria to reproduce the topology of the reaction from reactants to products; i.e., the calibration was not limited to the saddle point zone.

First, a kinetics study using variational transition-state theory (VTST) was performed. The thermal forward rate constants agreed with the experimental information over the temperature range 180−410 K, taking into account the experimental error bar. This agreement is obviously a consequence of the parametrization used, but it lends confidence to the new PES, and permits one to obtain the kinetic isotope effects (KIEs). Two sets of KIEs were calculated: F + CH_4/F + CD_4 and F + $HCHD_2$/F + DCH_2D. These showed reasonable agreement with experiment, taking into account the experimental error bar, and reproduced the experimental variation with temperature. Note that these results (forward rate constants, activation energy, and KIEs) represent a sensitive test of several macroscopic features of the new surface which are absent in other surfaces recently developed to analyze the title reaction. This information, although macroscopic, can be useful in dynamics analyses, because the barrier height, tunneling effect, activation energy, etc. inform one about the topology of the reactive system. The analysis of the reaction path curvature (kappa factor) showed qualitatively that large F−H stretching and small CH_3 umbrella bending vibrational excitations are expected in the products. This qualitative prediction agrees with the experimental evidence, and with the quantitative dynamics results in this paper.

Second, an exhaustive dynamics study employing quasiclassical trajectory (QCT) calculations was also performed on this PES. The product energy partition obtained reproduced the experimental behavior, although it overestimated the CH_3 coproduct internal energy and underestimated the relative traslational energy. The present PES remarkably improves the FH(v',j') product rovibrational distributions with respect to the previous PES-2005 surface, and showed better agreement with experiment.

Finally, the oscillatory pattern in the excitation function, the forward/backward predominance in the differential cross section analysis at 1.8 kcal mol^{-1}, and the dramatic changes in the DCS−Ecoll−θ 3D plot, are signatures of the resonance reported experimentally by Shiu et al.,[54] and assigned to wells in the vibrationally adiabatic curve as found in our surface. Obviously, the classical nature of the QCT calculations means that this conclusion is only tentative, and quantum-mechanical (QM) calculations will be required for a firmer conclusion to be drawn.

A comparison with very different surfaces recently constructed for the title reaction (interpolated ab initio and semiempirical SRP-PM3) showed that the accuracy of the polyatomic surfaces is today still far from the accuracy attained for triatomic systems. In particular, the dynamics results were strongly dependent on the PES construction.

In sum, our theoretical results showed good agreement with the experimental kinetics measurements (forward rate constants, activation energy, KIEs, and reaction path curvature), and moderately good agreement with the broad spectrum of experimental dynamics measurements (rovibrational excitation, available internal energy in products, and scattering distributions). This qualitative agreement lends support to the newly constructed polyatomic PES, although there are some differences which may be due to the potential energy surface, of course, but also to the known limitations of the QCT method and/or problems with the very sparse experimental data available for comparison.

Acknowledgment. This work was partially supported by the Junta de Extremadura, Spain (Project No. 2PR04A001).

References and Notes

(1) Corchado, J. C.; Espinosa-Garcia, J. *J. Chem. Phys.* **1996**, *105*, 3152.

(2) Rangel, C.; Navarrete, M.; Espinosa-Garcia, J. *J. Phys. Chem. A* **2005**, *109*, 1441.

(3) Castillo, J. F.; Aoiz, F. J.; Bañares, L.; Martinez-Nuñez, A.; Fernandez-Ramos, A.; Vazquez, S. *J. Phys. Chem. A* **2005**, *109*, 8459.

(4) Troya, D. *J. Chem. Phys.* **2005**, *123*, 214305.

(5) Troya, D.; Millan, J.; Baños, I.; Gonzalez, M. *J. Chem. Phys.* **2004**, *120*, 5181.

(6) Okuno, Y.; Yokohama, S.; Mashiko, S. *J. Chem. Phys.* **2000**, *113*, 3136.

(7) Roberto-Neto, O.; Machado, F. B. C.; Ornellas, F. R. *Chem. Phys.* **2005**, *315*, 27.

(8) (a) Persky, A. *J. Phys. Chem.* **1996**, 100, 689. (b) *Chem. Phys. Lett.* **1998**, *298*, 390; **1999**, *306*, 416 (erratum).

(9) Atkinson, R.; Baulch, D. L.; Cox, R. A.; Crowley, J. N.; Hampson, R. F.; Kerr, J. A.; Rossi, M. J.; Troe, J. *IUPAC Subcommittee on Gas Kinetic Data Evaluation*; February 2004.

(10) (a) Alexander, M. H.; Werner, H.-J.; Manolopoulos, D. E. *J. Chem. Phys.* **1999**, *109*, 4013. (b) Alexander, M. H.; Manolopoulos, D. E.; Werner, H.-J. *J. Chem. Phys.* **2000**, *113*, 11084.

(11) http://w3qf.unex.es/html/superficies.htm.

(12) (a) Gordon, M. S.; Truhlar, D. G. *J. Am. Chem. Soc.* **1986**, *108*, 5412. (b) Fast, P. L.; Corchado, J. C.; Sanchez, M. L.; Truhlar, D. G. *J. Phys. Chem. A* **1999**, *103*, 3139.

(13) Collins, M. A. *Theor. Chem. Acc.* **2002**, *108*, 313.

(14) Truhlar, D. G.; Isaacson, A. D.; Garrett, B. C. In *Theory of Chemical Reaction Dynamics*; Baer, M., Ed.; CRC Press: Boca Raton, FL, 1985; Vol. 4, p 65.
(15) Fast, P. L.; Truhlar, D. G. *J. Chem. Phys.* **1998**, *109*, 3721.
(16) Jackels, C. F.; Gu, Z.; Truhlar, D. G. *J. Chem. Phys.* **1995**, *102*, 3188.
(17) Chuang, Y.-Y.; Truhlar, D. G. *J. Phys. Chem. A* **1998**, *102*, 242.
(18) Garrett, B. C.; Truhlar, D. G.; Grev, R. S.; Magnuson, A. W. *J. Phys. Chem.* **1980**, *84*, 1730, **1983**, *87*, 4554 (erratum).
(19) Corchado, J. C.; Chuang, Y.-Y.; Fast, P. L.; Villa, J.; Hu, W.-P.; Liu, Y.-P.; Lynch, G. C.; Nguyen, K. A.; Jackels, C. F.; Melissas, V. S.; Lynch, B. J.; Rossi, I.; Coitiño, E. L.; Fernández-Ramos, A.; Steckler, R.; Garrett, B. C.; Isaacson, A. D.; Truhlar, D. G. *POLYRATE*, version 8.5.1; University of Minnesota: Minneapolis, MN, 2000.
(20) Chase, M. W.; Davis, C. A.; Downey, J. R.; Frurip, D. J.; McDonald, R. A.; Syverud, A. N. JANAF Thermochemical tables. *J. Phys. Chem. Ref. Data* **1985**, *Suppl. 14*.
(21) Porter, R. N.; Raff, L. M. In *Dynamics of Molecular Collisions, Part B*; Miller, W. H., Ed.; Plenum Press: New York, 1976.
(22) Truhlar, D. G.; Muckerman, J. T. In *Atom-molecules Collision Theory*; Bernstein, R. B., Ed.; Plenum Press: New York, 1979.
(23) Raff, L. M.; Thompson, D. L. In *Theory of Chemical Reaction Dynamics*; Baer, M., Ed.; CRC Press: Boca Raton, 1985; Vol. 3.
(24) Hase, W. L.; Duchovic, R. J.; Hu, X.; Komornicki, A.; Lim, K. F.; Lu, D.-h.; Peslherbe, G. H.; Swamy, K. N.; Van de Linde, S. R.; Varandas, A. J. C.; Wang, H.; Wolf, R. J. VENUS96: A General Chemical Dynamics Computer Program. *QCPE Bull.* **1996**, *16*, 43.
(25) Rangel, C.; Corchado, J. C.; Espinosa-Garcia, J. *J. Phys. Chem. A* **2006**, *110*, 10375.
(26) Bowman, J. M.; Kuppermann, A. *J. Chem. Phys.* **1973**, *59*, 6524.
(27) Truhlar, D. G. *J. Phys. Chem.* **1979**, *83*, 18.
(28) Schatz, G. C. *J. Chem. Phys.* **1983**, *79*, 5386.
(29) Lu, D.-h.; Hase, W. L. *J. Chem. Phys.* **1988**, *89*, 6723.
(30) Varandas, A. J. C. *Chem. Phys. Lett.* **1994**, *225*, 18.
(31) Ben-Nun, M.; Levine, R. D. *J. Chem. Phys.* **1996**, *105*, 8136.
(32) McCormack, D. A.; Lim, K. F. *Phys. Chem. Chem. Phys.* **1999**, *1*, 1.
(33) Stock, G.; Müller, U. *J. Chem. Phys.* **1999**, *111*, 65.
(34) Marques, J. M. C.; Martinez-Nuñez, E.; Fernandez-Ramos, A.; Vazquez, S. *J. Phys. Chem. A* **2005**, *109*, 5415.
(35) Duchovic, R. J.; Parker, M. A. *J. Phys. Chem. A* **2005**, *109*, 5883.
(36) Schatz, G. C.; Amaee, B.; Connor, J. N. L. *J. Chem. Phys.* **1990**, *92*, 4893.
(37) Troya, D.; Pascual, R. Z.; Schatz, G. C. *J. Phys. Chem. A* **2003**, *107*, 10497.
(38) Kuntz, P. J.; Nemeth, E. M.; Polanyi, J. C.; Rosner, S. D.; Young, C. E. *J. Chem. Phys.* **1966**, *44*, 1168.
(39) Miller, W. H.; Handy, N. C.; Adams, J. E. *J. Chem. Phys.* **1980**, *72*, 99.
(40) Morokuma, K.; Kato, S. In Potential Energy Surfaces and Dynamics Calculations, Ed. D. G. Truhlar Plenum: New York, 1981.
(41) Kraka, E.; Dunning, T. H. In *Advances in Molecular Electronic Structure Theory*; JAI: New York, 1990; Vol. I, p 129.
(42) (a) Parker, J. H.; Pimentel, G. C. *J. Chem. Phys.* **1969**, *51*, 91. (b) Jonathan, N.; Melliar-Smith, C. M.; Slater, D. H. *Mol. Phys.* **1971**, *20*, 93. (c) Chang, H. W.; Setser, D. W. *J. Chem. Phys.* **1973**, *58*, 2298. (d) Nazar, M. A.; Polanyi, J. C. *Chem. Phys.* **1981**, *55*, 299. (e) Manocha, A. S.; Setser, D. W.; Wickramaaratchi, M. A. *Chem. Phys.* **1993**, *76*, 129. (f) Wickramaaratchi, M. A.; Setser, D. W.; Hildebrant, H.; Korbitzer, B.; Heydtmann, H. *Chem. Phys.* **1985**, *94*, 109. (g) Harper, W. H.; Nizkorodov, S. A.; Nesbitt, D. J. *J. Chem. Phys.* **2000**, *113*, 3670.
(43) Sugawara, K.; Ito, F.; Nakanaga, T.; Takeo, H.; Matsumura, Ch. *J. Chem. Phys.* **1990**, *92*, 5328.
(44) Foon, R.; Reid, G. P.; Tait, K. B. *J. Chem. Soc., Faraday Trans.* **1972**, *68*, 1131.
(45) Williams, R. L.; Rowland, F. S. *J. Phys. Chem.* **1973**, *77*, 301.
(46) Wallington, T. J.; Hurley, M. D. *Chem. Phys. Lett.* **1992**, *193*, 84.
(47) Persky, A. *Chem. Phys. Lett.* **2006**, *430*, 251.
(48) Persky, A. *J. Chem. Phys.* **1974**, *60*, 49.
(49) Zhou, J.; Lin, J. J.; Shiu, W.; Pu, S. C.; Liu, K. *J. Chem. Phys.* **2003**, *119*, 2538.
(50) Kornweitz, H.; Persky, A.; Levine, R. D. *Chem. Phys. Lett.* **1998**, *289*, 125.
(51) Shiu, W.; Lin, J. J.; Liu, K.; Wu, M.; Parker, D. H. *J. Chem. Phys.* **2004**, *120*, 117.
(52) Tully, J. C. *J. Chem. Phys.* **1974**, *60*, 3042.
(53) Aoiz, F. J.; Bañares, L.; Castillo, J. F. *J. Chem. Phys.* **1999**, *111*, 4013.
(54) Shiu, W.; Lin, J. J.; Liu, K. *Phys. Rev. Lett.* **2004**, *92*, 103201.
(55) Wang, Q.; Cai, Z.; Feng, D. *J. Mol. Struct. (THEOCHEM)* **2006**, *759*, 31.
(56) Chu, T.; Zhang, X.; Ju, L.; Yao, L.; Han, K.-L.; Wang, M.; Zhang, J. Z. H. *Chem. Phys. Lett.* **2006**, *424*, 243.
(57) Harper, W. W.; Nizkorodov, S. A.; Nesbitt, D. J. *Chem. Phys. Lett.* **2001**, *335*, 381.
(58) Newmark, D. M.; Wodtke, A. M.; Robinson, G. N.; Hayden, C. C.; Lee, Y. L. *J. Chem. Phys.* **1985**, *82*, 3045.
(59) Lee, S. H.; Dang, F.; Liu, K. *J. Chem. Phys.* **2006**, *125*, 133106.
(60) Zhang, B.; Liu, K. *J. Chem. Phys.* **2005**, *122*, 101102.